JOURNAL OF VIROLOGY, Nov. 1998, p. 8988–9001 Vol. 72, No. 11
0022-538X/98/$04.00+0

African Swine Fever Virus Is Enveloped by a Two-Membraned Collapsed Cisterna Derived from the Endoplasmic Reticulum

GERMÁN ANDRÉS, RAMÓN GARCÍA-ESCUDERO, CARMEN SIMÓN-MATEO, AND ELADIO VIÑUELA*

Centro de Biología Molecular "Severo Ochoa" (Consejo Superior de Investigaciones Científicas-Universidad Autónoma de Madrid), Facultad de Ciencias, Universidad Autónoma de Madrid, Cantoblanco, 28049 Madrid, Spain

Received 22 May 1998/Accepted 30 July 1998

During the cytoplasmic maturation of African swine fever virus (ASFV) within the viral factories, the DNA-containing core becomes wrapped by two shells, an inner lipid envelope and an outer icosahedral capsid. We have previously shown that the inner envelope is derived from precursor membrane-like structures on which the capsid layer is progressively assembled. In the present work, we analyzed the origin of these viral membranes and the mechanism of envelopment of ASFV. Electron microscopy studies on permeabilized infected cells revealed the presence of two tightly apposed membranes within the precursor membranous structures as well as polyhedral assembling particles. Both membranes could be detached after digestion of intracellular virions with proteinase K. Importantly, membrane loop structures were observed at the ends of open intermediates, which suggests that the inner envelope is derived from a membrane cisterna. Ultraestructural and immunocytochemical analyses showed a close association and even direct continuities between the endoplasmic reticulum (ER) and assembling virus particles at the bordering areas of the viral factories. Such interactions become evident with an ASFV recombinant that inducibly expresses the major capsid protein p72. In the absence of the inducer, viral morphogenesis was arrested at a stage at which partially and fully collapsed ER cisternae enwrapped the core material. Together, these results indicate that ASFV, like the poxviruses, becomes engulfed by a two-membraned collapsed cisterna derived from the ER.

African swine fever virus (ASFV) is a complex enveloped deoxyvirus with unique features among the DNA-containing viruses (9, 44). Large DNA viruses include families of icosahedral viruses (*Herpesviridae* and *Iridoviridae*) and brick-shaped viruses (*Poxviridae*). ASFV does not fit well into any of these groups because, although its genome structure is similar to that of poxviruses (17, 39), its icosahedral structure is like that of iridoviruses (2, 7). So far, ASFV is the only member of an unnamed family of animal DNA viruses (12). The viral genome is a single molecule of double-stranded DNA that, in the case of the avirulent strain BA71V, comprises about 150 open reading frames (45). The viral particle contains more than 30 different polypeptides (6) and, in spite of being an enveloped virus, lacks major glycoproteins (11). At least six of the major ASFV structural proteins (p150, p37, p35, p34, p15, and p14) are synthesized as polyprotein precursors (pp220 and pp62), which is an unusual feature in a DNA virus (36, 37).

The virus particle possesses a complex structure formed by several concentric domains with an overall icosahedral shape and a diameter of about 200 nm (7). The viral core is composed of a DNA-containing nucleoid enclosed by a thick protein layer, the core shell, which contains the mature products derived from polyprotein pp220 (3). The core is successively surrounded by a inner lipid envelope, a capsid formed by protein subunits arranged in a hexagonal lattice, and, finally, an outer lipid envelope acquired by budding at the cell surface (3, 4, 7). ASFV morphogenesis takes place in discrete cytoplasmic areas, the viral factories, where the replication of the viral DNA also occurs (3–5, 14, 23). These areas contain abundant membrane-like structures, which represent the first morphological evidence of virus assembly. Viral membranes engulf the core material while acquiring a polyhedral shape by the assembly of the outer capsid layer (3). To facilite the study of ASFV assembly, we have recently developed a system for inducible gene expression from ASFV recombinants (15). Using this approach, we showed that the formation of the capsid on the inner envelope is a progressive process depending on expression of protein p72, the major component of the capsid.

In the present study, we have focused our attention to the origin and the mechanism of acquisition of the inner viral envelope. In general, enveloped viruses acquire their membranes from specific host cell compartments where certain viral membrane proteins are targeted (19, 26, 40). Envelopment usually takes place through a budding process whereby the virus particle is wrapped by a single membrane and leaves its original compartment. However, a striking exception has arisen in recent studies on the assembly of two large DNA-containing viruses, the poxviruses and the herpesviruses. For both of these classes, it has been shown that the viruses become enwrapped by cellular membrane cisternae, thus acquiring two lipid membranes in a single step (16, 29, 33, 38, 43). With regard to ASFV, a recent report by Cobbold et al. (8) has suggested that ASFV is enveloped by the endoplasmic reticulum (ER). Such a proposal was based on indirect data such as the comigration in sucrose gradients of viral protein p72 with the luminal ER marker protein disulfide isomerase (PDI) and on the apparent colocalization of PDI with the viral factories in immunofluorescence experiments.

In the present work, we provide morphological and immunocytochemical evidence showing that the ASFV inner envelope is indeed composed of two juxtaposed membranes derived

* Corresponding author. Mailing address: Centro de Biología Molecular "Severo Ochoa," Facultad de Ciencias, Universidad Autónoma de Madrid, Cantoblanco, 28049 Madrid, Spain. Phone: 34 91 397 84 36. Fax: 34 91 397 84 90. E-mail: Evinuela@mvax.cbm.uam.es.

from an ER cisterna. A new model for the structure and assembly pathway of ASFV is therefore presented.

MATERIALS AND METHODS

Cells and viruses. Vero cells (ATCC CCL81) were cultured in Dulbecco's modified Eagle's medium supplemented with 10% newborn calf serum, which was reduced to 2% during viral infection. The ASFV strain BA71V, adapted to grow in Vero cells, has been described previously (13). Highly purified extracellular ASFV was obtained by Percoll equilibrium centrifugation (6). The recombinant virus vA72, which inducibly expresses the major capsid protein p72 (15), was propagated in the presence of 2 mM isopropyl-β-D-thiogalactopyranoside (IPTG). Infections with parental BA71V and recombinant vA72 viruses were carried out at a multiplicity of infection of 10 PFU/cell.

Antibodies. Rabbit polyclonal serum and mouse monoclonal antibody (MAb) 24A.G4 against the ASFV proteins pp220/p150 have been described previously (32, 36). Rabbit antiserum against PDI was kindly provided by J. G. Castaño (Instituto de Investigaciones Biomédicas, Madrid, Spain) (24). Mouse MAb and rabbit serum against ER membrane protein p63 were obtained from A. Schweizer and J. Rohrer (Biocenter, Basel, Switzerland) (35). Rabbit serum against membrane ER glycoproteins (anti-MERG) was a gift from D. I. Meyer (University of California, Los Angeles, Calif.) (27). Rabbit antiserum against galactosyltransferase was a gift from Eric Berger (Physiologisches Institut, Zurich, Switzerland) (30). Mouse MAb against membrane protein p53 was kindly provided by H.-P. Hauri (Biocenter, Basel, Switzerland) (34). MAb 25H8 against the *cis*-Golgi network membrane protein gp74 (1) and rabbit serum to the *cis-medial*-Golgi protein gp100 (46) were kindly provided by I. Sandoval (Centro de Biología Molecular "Severo Ochoa," Madrid, Spain). Mouse MAb 1D3 against PDI was obtained from Stressgene Biotechnologies Corp. (Victoria, British Columbia, Canada) (42), and rabbit serum against cathepsin L was obtained from BioAss (Diessen, Germany).

Light microscopy. Vero cells were grown to ca. 70% confluency in chamber slides (Lab-Tek, Nunc) and then infected at 1 PFU per cell with ASFV BA71V. For immunofluorescence labeling, the cells were fixed after the indicated times with methanol at −20°C for 5 min. For staining of the *trans*-Golgi network, the cells were fixed with 3% paraformaldehyde for 15 min at room temperature and incubated with C_6-NBD-ceramide (Molecular Probes Inc., Eugene, Oreg.) as previously described (25). Double-labeling experiments were performed by incubating together the two primary antibodies and, subsequently, the two secondary antibodies at 37°C for 1 h. As a control, each antibody was tested individually. The secondary antibodies Texas red-linked donkey anti-rabbit, Texas red-linked sheep anti-mouse, and fluoresceinated donkey anti-rabbit antibodies were obtained from Amersham Life Science. The fluoresceinated goat anti-mouse immunoglobulin G was obtained from Tago Inc. (Burlingame, Calif.). The coverslips were mounted on glass slides with Moviol, examined with an Axiovert fluorescence microscope (Carl Zeiss, Inc., Oberkochen, Germany), and photographed with Kodak film (TMAX; ASA 400).

Electron microscopy (EM). For conventional Epon section analysis, ASFV-infected Vero cells were fixed with 2% glutaraldehyde–2% tannic acid in 200 mM cacodylate buffer (pH 7.4) at room temperature for 1 h. Postfixation was carried out with 1% OsO_4 and 1.5% $K_3Fe(CN)_6$ in cacodylate buffer at 4°C for 30 min. After extensive washing with distilled water, the samples were dehydrated and embedded in Epon.

Infected cells were permeabilized with the bacterial toxin streptolysin O (SLO) as described by Sodeik et al. (38) with minor modifications. Briefly, infected Vero cell monolayers were incubated on ice with 8 U of SLO (Sigma) per ml for 15 min. After extensive washing, the cells were incubated at 37°C for 30 min to allow pore formation and then processed for Epon embedding.

For both cryosectioning and freeze-substitution, the infected cells were fixed on the culture dish with 8 or 4% formaldehyde and 0.1% glutaraldehyde in 200 mM HEPES (pH 7.2) for 1 h at room temperature. After fixation, the cells were carefully scraped with a rubber policeman and centrifuged at 1,500 × *g* for 3 min. The cell pellets were embedded in 10% gelatin from cold water fish skin (Sigma), cut into 1-mm^3 pieces, and then infused with a mixture containing 10% polyvinylpyrrolidone (10 kDa; Sigma) and 2.07 M sucrose. Sample blocks were frozen and stored in liquid nitrogen before use.

Ultrathin cryosections were obtained at around −110°C with a Reichert-Jung Ultracut E apparatus (Leica, Vienna, Austria) equipped with a 35° diamond knife and an antistatic device (Diatome, Biel, Switzerland). Section retrieval was performed by the method of Liou et al. (21). For this, the sections were picked up with a mixture of 2% aqueous methylcellulose (25 cP; Sigma) and 2.3 M sucrose in 1:1 proportion. After being thawed, the sections were transferred onto carbon-coated Formvar films on copper grids. Immunolabeling, drying, and contrasting of the sections were performed as described by Griffiths (18).

Freeze-substitution was carried out with Leica AFS system KF80. Sample blocks were incubated at −90°C for 40 h in methanol supplemented with 0.5% tannic acid. Dehydration was continued with pure methanol by raising the temperature to −35°C at a rate of 3°C/h. Finally, the samples were embedded in Lowicryl K4M at −35°C and polymerized by irradiation with UV light. Immunogold labeling of freeze-substituted samples was performed essentially as described previously (3). The PDI labeling with MAb 1D3 was amplified with a rabbit anti-mouse immunoglobulin G (Dako, Copenhagen, Denmark) followed by protein A-gold complexes (diameter, 15 nm; BioCell Research Laboratories, Cardiff, United Kingdom). For the double-labeling experiment, the sections were sequentially incubated with the serum to pp220/p150 followed by protein A-gold (diameter, 10 nm) and with the anti-PDI MAb followed by protein A-gold (diameter, 15 nm). Between the two steps, the sections were fixed with 1% glutaraldehyde for 5 min and then incubated with 100 mM glycine in phosphate-buffered saline (PBS) for 5 min.

For negative staining of ASFV, purified virus particles were adsorbed to glow-discharged, Formvar-coated nickel grids, rinsed briefly with PBS, and fixed with 2% glutaraldehyde for 5 min. Finally, the virions were negatively stained with 2% phosphotungstic acid for 5 min.

Detergent and protease treatments of virus particles. Suspensions of highly purified virions in PBS were incubated with 0.5% β-D-octylglucopyranoside or 0.5% Nonidet P-40 in PBS for 5 min at room temperature. After the treatment, the virus particles were sedimented in a Beckman Airfuge at 100,000 × *g* for 5 min, fixed with 2% glutaraldehyde for 1 h, and processed for Epon embedding.

For protease treatment of intracellular virions, infected Vero cells were perforated at 20 h postinfection (p.i.) by hypotonic lysis as previously described (38). The broken cells were centrifuged at 1,000 × *g* for 5 min and resuspended for 30 min in 0.25 M sucrose–25 mM HEPES (pH 7.2)–5 mM magnesium acetate–50 mM potassium acetate containing 5 mg of proteinase K (Merck, Darmstadt, Germany) per ml. Finally, the samples were centrifuged at 3,000 × *g* for 5 min, rinsed twice with PBS, fixed with 2% glutaraldehyde for 1 h, and processed for Epon embedding.

To estimate the size of nontreated or detergent-treated virions, the measurements were made on micrographs of particles showing hexagonal outlines in threefold projections. The lengths were estimated from side to side and expressed as means and standard deviations. The mean diameter of the proteinase-treated particles was calculated by using particles with an apparently intact core containing a nucleoid of about 80 nm. The measurements were typically performed on magnifications of ×150,000.

Specimens were examined with a JEOL 1010 or JEOL 1200X electron microscope.

RESULTS

The inner envelope of ASFV is a double-membrane domain. Figure 1A to C show extracellular ASFV particles processed by three different EM methods: conventional Epon embedding (Fig. 1A), cryosectioning (Fig. 1B), and negative staining of whole particles (Fig. 1C). All these images show that ASFV consists of a core surrounded by three concentric shells with an overall icosahedral shape. However, the nature of these layers can be differently interpreted depending on the technique used. Thus, all of them look usually like lipid membranes in both Epon sections and cryosections. However, the intermediate layer, as visualized by negative staining, clearly shows the regular array of globular protein units composing the viral capsid (Fig. 1C). Therefore, we interpret these three layers as an inner lipid envelope, a protein capsid, and an outer lipid envelope (Fig. 1A to C). It is well established that the outermost envelope is a single lipid membrane acquired by budding at the cell surface (4). The first goal of the present study was to determine the nature of the innermost envelope.

To obtain a better visualization of the membrane profiles, the infected cells were usually permeabilized at 18 to 24 h p.i. with the bacterial toxin SLO or by hypotonic lysis. Figure 1D to J show ultrathin Epon sections of different virus assembly intermediates present within the cytoplasmic viral factories. In agreement with our previous observations (3), ASFV particles were found to assemble from precursor membrane-like structures (Fig. 1D), which became polyhedral particles by the gradual assembly of the outer capsid on one of their two faces (Fig. 1E). Concomitantly, the electron-dense core material appeared to associate with their opposite faces (Fig. 1E). Since the inner viral envelope is derived directly from the precursor membranous structures and the entire assembly process occurs in the viroplasm, cytosolic ambient ASFV envelopment cannot be explained by a budding process at a cellular organelle. We therefore explored the possibility that ASFV becomes engulfed by a cellular cisterna, thus acquiring two lipid membranes simultaneously.

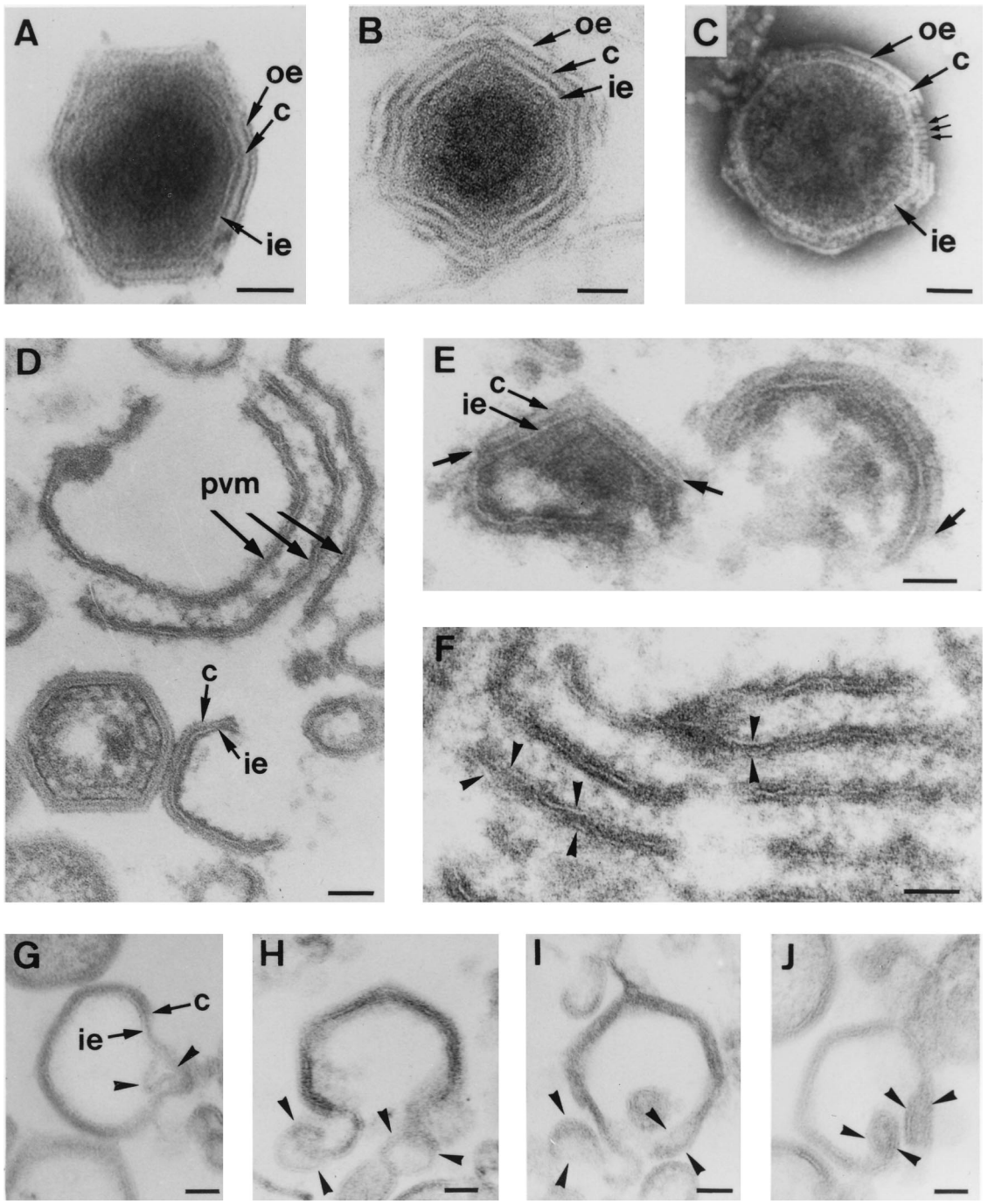

FIG. 1. Structure and assembly of ASFV. (A to C) Extracellular ASFV particles processed by Epon sectioning (A), cryosectioning (B), and negative staining (C). All these EM methods reveal an overall structure consisting of a central core surrounded by three layers: the inner envelope (ie), the capsid (c), and the outer envelope (oe). Note that in the negatively stained particle, individual capsomers (small arrows in panel C) are evident within the capsid. (D to J) Ultrathin Epon sections of viral intermediates from infected Vero cells permeabilized at 18 to 24 h p.i. Intracellular ASFV particles mature from precursor viral membranous structures (pvm) present in the viral factories (D), which become polyhedral particles by the gradual formation of the capsid on one of their faces (D and E). The short arrows in panel E indicate the limits of capsids assembling on the inner envelopes. Note also the electron-dense core material underneath the concave side of the inner envelope (E). Close inspection of the assembly intermediates revealed two distinct membranes within the precursor membranous structures (arrowheads in panel F) as well as in polyhedral assembling particles (arrowheads in panels G to J). Note that the ends of open particles (H to J) appeared as membrane loops, which suggests that ASFV becomes enwrapped by a collapsed two-membraned cisterna. Bars, 50 nm.

Inspection of the precursor membranous forms revealed that despite their trilaminar appearance, they were markedly different from the host cell membranes because of their higher electron density and thickness (around 12 nm) and the usual presence of electron-dense spicules covering their faces (Fig. 1D). Most importantly, two tightly apposed membranes were often detected within these precursor structures (Fig. 1F). A similar finding was made during the examination of assem-

bling polyhedral particles. Occasionally, the inner envelope appeared to locally separate into two distinct lipid bilayers (Fig. 1G). More frequently, membrane loops were observed at the ends of open intermediates (Fig. 1H to J). Together, these observations argue that the inner envelope is derived from a collapsed two-membraned cisterna.

To further investigate the existence of two lipid membranes within intracellular particles, we tested the action of proteinase K on the viral structure. For this purpose, permeabilized infected cells were incubated with the proteinase and then processed for Epon embedding. After this treatment, most of the virus particles present in the viral factories exhibited pronounced changes in their icosahedral morphology. Compared with nontreated intracellular virions (Fig. 2A), it was evident that the virions incubated with the proteinase had lost the outer layer, i.e., the capsid, but not the inner envelope (Fig. 2B). Furthermore, the envelope appeared partially dissociated into two membrane layers within highly disrupted particles (Fig. 2C to E).

In another approach, purified extracellular virions were incubated with the nonionic detergent β-D-octylglucoside (Fig. 2F and G) or Nonidet P-40 (data not shown). After these treatments, the outer and inner lipid envelopes were removed and the core structure was partially altered (compare Fig. 2F and G with Fig. 1A to C and 2A). However, the capsid remained apparently intact and the resulting particles retained their polyhedral shape, which demonstrates the central role of this outer layer in the virus symmetry. Additional support for these observations was obtained by comparing the sizes of the particles resulting from the different treatments. Thus, while the average diameter of the proteinase-treated virions (148 ± 6 nm, $n = 15$) was clearly smaller than that of nontreated intracellular particles (170 ± 7 nm, $n = 25$), the size of the particles obtained after the detergent incubation (166 ± 7 nm, $n = 15$) was not significantly different.

In summary, these findings are in agreement with the lipid nature of the inner shell and the protein nature of the outer one. Furthermore, they support the existence of two tightly apposed membranes within the envelope of the intracellular ASFV particles, which is consistent with their being wrapped by a membrane cisterna.

Relationship of ASFV assembly sites to cellular compartments. To analyze the origin of the ASFV inner envelope, our first step was to explore the possible colocalization of a set of well-characterized markers of cell organelles with the viral factories. For this, double-immunofluorescence experiments were performed on infected Vero cells fixed at 14 to 16 h p.i. The location of viral factories was determined with specific antibodies to ASFV polyprotein pp220 (32, 36) (Fig. 3B, D, F, and H). The ER was visualized with a MAb (42) (results not shown) and a polyclonal serum (24) (Fig. 3A) against the luminal marker PDI, the membrane protein p63 (35) (results not shown), the membrane marker of the intermediate compartment p53 (34) (results not shown), and a purified extract of membrane ER glycoproteins (anti-MERG [27]) (Fig. 3C). All the tested ER markers were essentially excluded from the cytoplasmic viral factories. However, it was evident that the ER labeling closely encompassed the assembly sites (compare Fig. 3A and C with Fig. 3B and D, respectively).

Similar results were obtained with antibodies against the Golgi membrane proteins gp74 (1) (Fig. 3E), gp100 (46) (results not shown), and galactosyltransferase (30) (Fig. 3G). Although these proteins did not colocalize with polyprotein pp220, their presence in the boundaries of the assembly sites was clear (compare Fig. 3E and G with Fig. 3F and H, respectively). Finally, no colocalization was observed with the markers to the endocytic-lysosomal pathway, C_6-NBD-ceramide and cathepsin L (results not shown). Together, these results indicate a virtual exclusion of the host cell organelles from the assembly sites.

We next examined the relationship between cellular organelles and viral structures at the EM level. As shown in Fig. 4A, the viral factories were closely surrounded by ER cisternae and by an enlarged Golgi apparatus, thus confirming the results of the immunofluorescence experiments and previous work (23). This observation led us to analyze possible interactions between host cell membranes and viral structures at the peripheral areas of the assembly sites. Such examination revealed frequent interactions between ER cisternae and the precursor viral membranous structures through viroplasmic electron-dense material (Fig. 4B). Most important, however, was the occasional finding of collapsed ER membranes in the close vicinity of (Fig. 4C) and even in direct continuity with (Fig. 4D) assembling virions. No interactions were apparent between viral intermediates and the Golgi complex. Collectively, these observations argue that viral membranes are derived from ER membranes.

ASFV zipper-like structures. Inspection of the areas contiguous with the assembly sites revealed the presence of a minor subpopulation of atypical viral structures (Fig. 5A). These viral forms which we refer to as zipper-like structures, seemed to consist of two ER cisternae bound by an extended and electron-dense viral domain structurally similar to the core shell (see below). To elucidate the unusual structure of these viral intermediates, two different approaches were undertaken. On the one hand, we examined the zipper-like structures of infected cells permeabilized with SLO. By this method, the soluble contents of the cytosol were extracted but the luminal contents, which were now easily identifiable, were not extracted (Fig. 5B). Under these conditions, the core shell appeared unequivocally limited by the luminal spaces of adjacent ER cisternae, thus confirming the previous interpretation. In the other aproach, the zipper-like structures were analyzed by using serial sections. As deduced from Fig. 5C, the viral domain is a laminar structure whose limiting surfaces are bound to the cytoplasmic sides of the ER membranes. Together, these finding confirm the interaction of ASFV structures with ER membranes.

A closely related type of zipper-like structures was also found within the viral factories. When comparing the marginal (Fig. 6A and B) and internal (Fig. 6C to F) zipper-like structures, it was evident that, in the latter case, the core shell was limited by two typical viral membrane-like structures (Fig. 6D). Moreover, a close examination revealed the existence of two apposed membranes within each viral envelope, as well as loop structures at their ends (Fig. 6E and F). Collectively, these findings argue again that viral envelopes are derived from collapsed ER cisternae. Eventually, the zipper-like intermediates became polyhedral structures (Fig. 6G to K). As with normal ASFV particles, this process was found to be a direct consequence of the progressive assembly of an outer capsid on one of the limiting envelopes (Fig. 6G and H). Thus, the resulting closed icosahedral particles contained an extra inner envelope beneath the core shell. In a minor proportion of these double-enveloped particles, an electron-dense material appeared to be encapsidated to give rise to a nucleoid-like domain (Fig. 6I to K).

Together, these observations show the existence of an alternative assembly pathway leading to the formation of a minor and structurally distinct class of ASFV particles. It is noteworthy that the external layers, and even the core shell, of such particles seem to be morphologically identical to the corresponding domains of normal virions (3) (compare Fig. 2A and

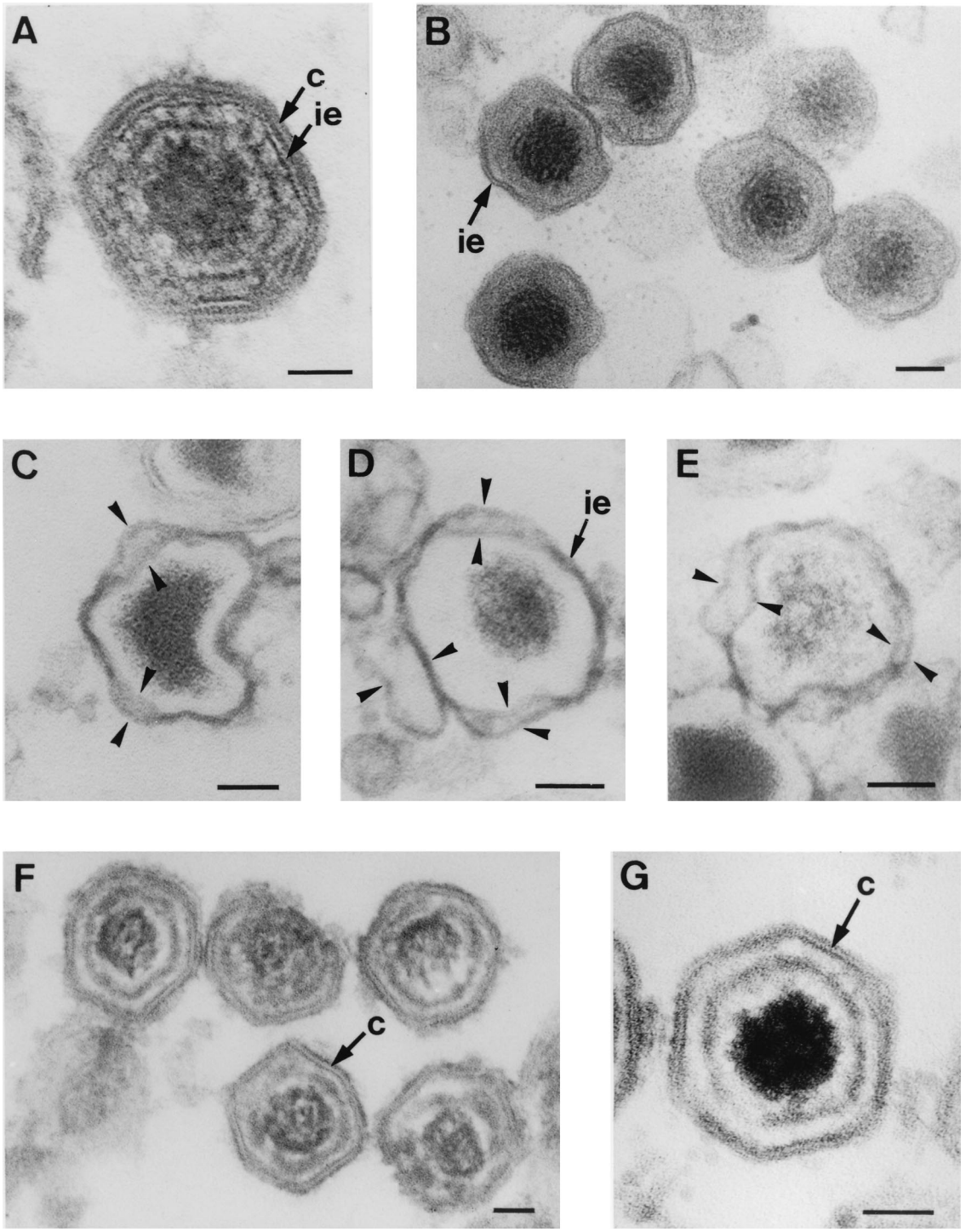

FIG. 2. Selective disruption of ASFV particles. (A) Epon section of an intact intracellular particle showing the central core successively enclosed by the inner envelope (ie) and the outer capsid (c). (B to E) Epon sections of intracellular virions incubated with proteinase K. At 20 h p.i. infected Vero cells were perforated by hypotonic lysis and subsequently incubated with proteinase K for 30 min at room temperature. After the proteinase treatment, intracellular particles had lost the capsid but not the inner envelope (B). Importantly, in highly damaged virions the inner envelope appeared dissociated in two distinct membranes (arrowheads in panels C to E). Note also the dramatic alteration of their icosahedral morphology. (F and G) Epon sections of purified extracellular particles treated for 30 min with the nonionic detergent β-D-octylglucopyranoside. Note the lack of the outer and the inner envelopes and the partial disruption of the viral core. Note also that the capsid remains apparently intact and the resulting particles retain their polyhedral shapes. Bars, 50 nm.

6K). Likewise, the apparent mechanisms of acquisition of the inner envelope, by wrapping from ER cisternae, and of the outer capsid, by a gradual building process, are also consistent with the assembly model described for normal particles. Whether the unusual double-enveloped virions are also infectious remains to be answered.

Immunolocalization of ER proteins within viral structures. To confirm the cellular origin of the viral envelopes, we per-

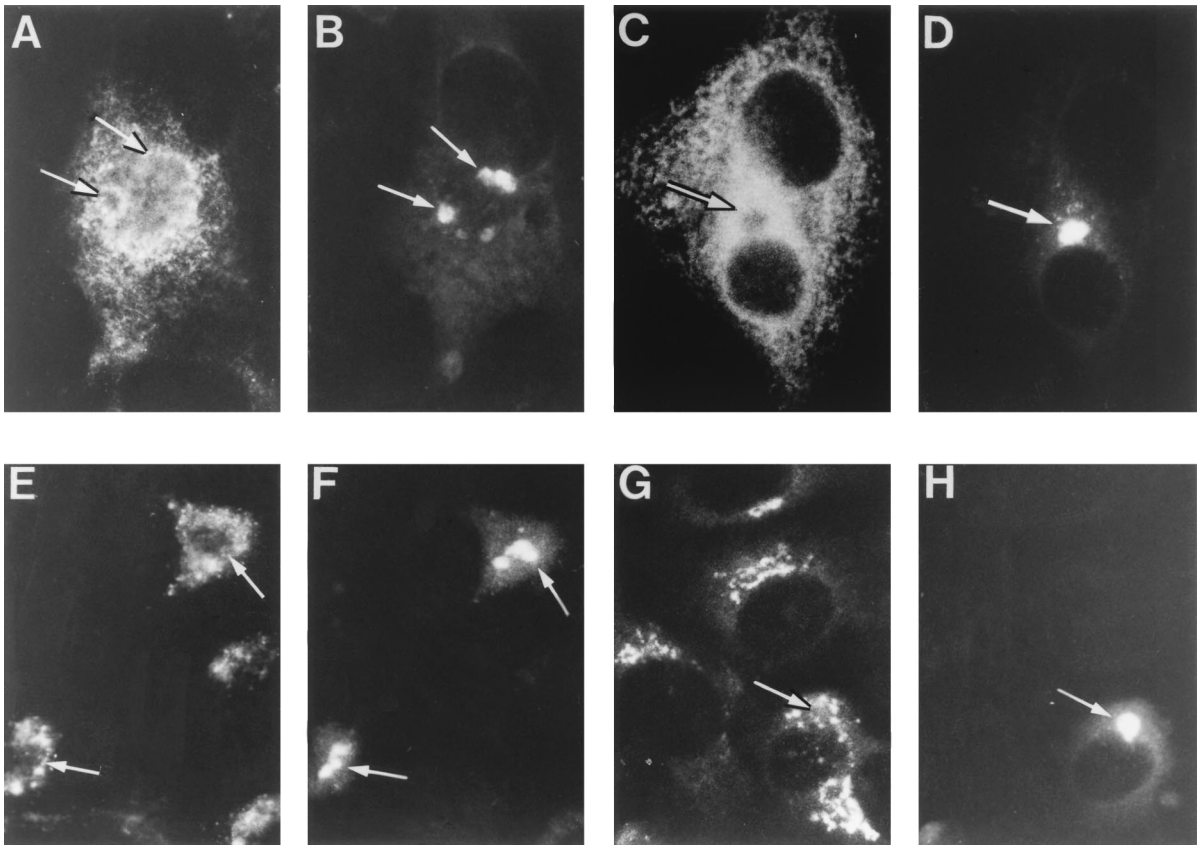

FIG. 3. Immunofluorescence analysis of ER and Golgi marker proteins in ASFV-infected cells. Infected Vero cells were fixed at 12 to 16 h p.i. with methanol at −20°C. Double-labeling experiments were performed with antibodies to ASFV polyprotein pp220 to stain the viral factories (B, D, F, and H) and with antibodies to different ER and Golgi proteins (A, C, E, and G), as follows. For ER labeling, a rabbit antiserum to the luminal marker PDI (A) and a rabbit antiserum to membrane ER glycoproteins (C) were used. For Golgi labeling, a MAb to the membrane glycoprotein gp74 (E) and a rabbit serum to galactosyltransferase (G) were used. The antibodies to pp220 were a mouse MAb (24A.G4) (B, D, and H) and the rabbit antiserum anti-pp220/p150 (F). Double labeling was developed with fluorescein-coupled secondary antibodies for the assembly sites and Texas red-conjugated antibodies for the organelle markers. Note that viral factories (arrows) essentially exclude the ER and Golgi markers but are closely encompassed by them.

formed immunogold labeling with antibodies to ER proteins on sections of infected cells processed at 18 h p.i. for freeze-substitution (Fig. 7A to C) or cryosectioning (Fig. 7D and E). As shown in Fig. 7A, the labeling with antibodies to the luminal protein PDI was virtually excluded from the assembly sites. However, a strong signal was observed in the intracisternal spaces of marginal zipper-like structures (Fig. 7B). The mixted cellular and viral nature of these intermediates was confirmed by double-labeling experiments with antibodies to the ER protein PDI and to ASFV polyprotein pp220, which has been shown previously to localize within the viral core shell (3). As shown in Fig. 7C, whereas the luminal contents was labeled with anti-PDI antibodies, the viral domains were labeled with the anti-pp220 serum. On the other hand, the serum against membrane ER glycoproteins showed low but significant labeling associated with virus intermediates within the assembly sites (Fig. 7D) and strong labeling on the membranes of marginal zipper-like structures (Fig. 7E).

As mentioned in the introduction, a recent study by Cobbold et al. (8) has suggested colocalization of PDI with the viral factories on the basis of immunofluorescence experiments. Close examination of the reported photograph (Fig. 7 of reference 8) reveals that anti-PDI labeling was surprisingly much more intense within the assembly sites than in the surrounding cytoplasm. Such a location is not supported by our findings obtained with the same MAb and other ER markers by both immunofluorescence and immuno-EM.

Recombinant vA72 intermediates are enwrapped by collapsed ER cisternae. We have recently shown that the zipper-like structures can be accumulated after infection with a recombinant virus, vA72, which inducibly expresses the major capsid protein p72 (15). Such a recombinant is IPTG dependent, and in the absence of the inducer, ASFV assembly is arrested at a stage where capsid formation is inhibited and most of the precursor membranes form zipper-like intermediates (15). We therefore took advantage of these observations to analyze the process of viral envelopment. To produce large amounts of zipper-like structures, Vero cells were infected with recombinant virus vA72 for 18 h in the absence of IPTG. After this period, the cells were processed by conventional Epon embedding. As shown in Fig. 8A, the assembly sites showed a virtual absence of icosahedral virus particles but a great accumulation of zipper-like structures. Importantly, these intermediates appeared clearly associated with ER cisternae at the boundaries of the viral factories (Fig. 8A and B). Moreover, such ER cisternae appeared often collapsed by the apposition of the limiting membranes and the subsequent constriction of the luminal spaces (Fig. 8C).

After 8 h of IPTG induction, the zipper-like structures became polyhedral forms by the progressive de novo assembly of

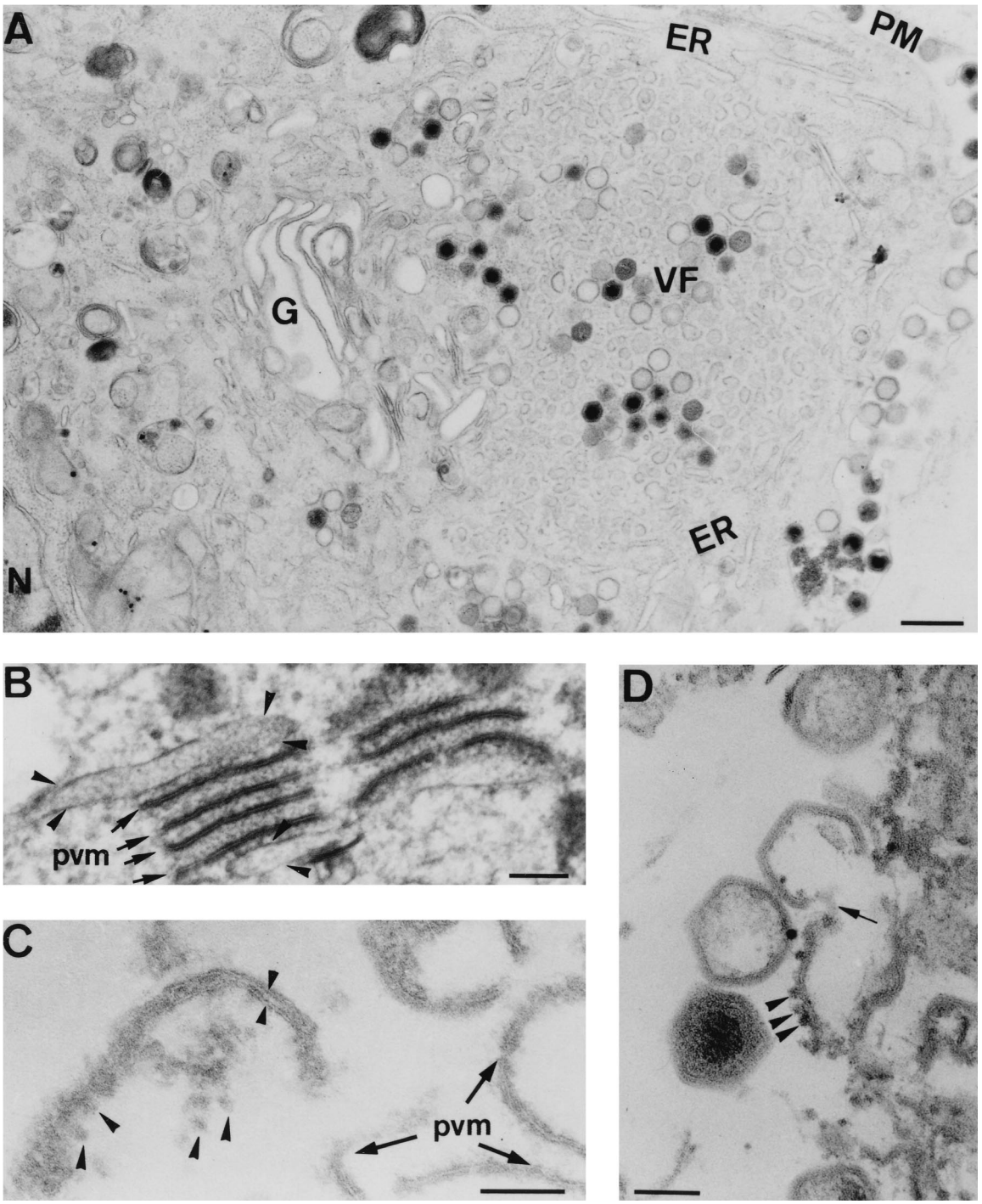

FIG. 4. Relationship between viral membranes and ER membranes. Ultrathin Epon sections of ASFV-infected Vero cells at 24 h p.i. are shown. (A) Viral factories (VF) were usually encompassed by an enlarged Golgi complex (G) and ER cisternae (ER). The plasma membrane (PM) and the nucleus (N) are also indicated. (B to D) At the limits of the assembly sites, a close association between ER membranes and viral structures was often evident. (B) Several precursor viral membranes (pvm, arrows) are present between two cellular cisternae (arrowheads). Note the presence of electron-dense viroplasmic material associated with both viral and cellular membranes. (C) An apparently collapsed ER cisterna (small arrowheads) with attached ribosomes (large arrowheads) is in close vicinity to precursor viral membranes. (D) Eventually, direct continuities (arrow) between membranes with attached ribosomes (arrowheads) and assembling virions were also evident. Bars: 500 nm (A), 100 nm (B to D).

the capsid layer on their external surfaces (Fig. 8D). As occurs with parental virus infections, evidence of the cisternal structure of the limiting envelopes was eventually detected at their ends, in the form of membrane loops. As recently described, a further evolution of these intermediates led to the assembly of closed double-enveloped icosahedral particles (15).

Collectively, these observations support the conclusion that ASFV inner envelopes originate from the collapse of the ER

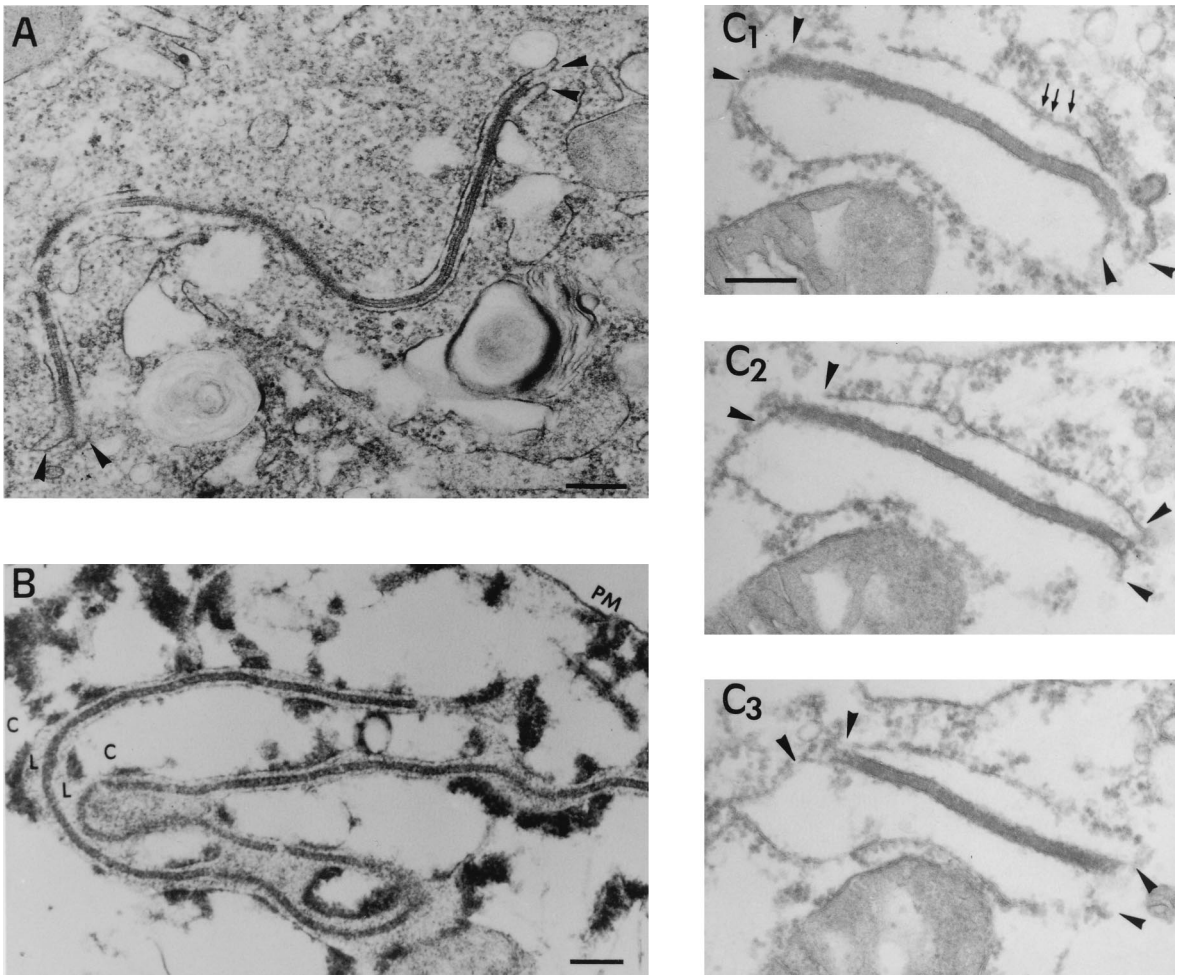

FIG. 5. Topology of the zipper-like structures. (A and B) Ultrathin Epon sections of marginal zipper-like structures within a nonpermeabilized (A) or SLO-permeabilized (B) infected cell at 16 h p.i. Note in the control (A) how the limits of the viral intermediate appear to be continuous with two adjacent ER cellular cisternae (arrowheads). After cell permeation (B), the cytosol (C) is extracted but not the luminal contents (L), which become obvious. Thus, it is clear that the core shell is a cytosolic structure limited by two ER cisternae. (C_1 to C_3) Set of serial sections of a peripheral zipper-like structure. The core shell is interpreted as a laminar structure whose limiting surfaces interact with the cytoplasmic sides of ER cisternae. Note the presence of ribosomes (small arrows) attached to ER membranes (arrowheads). Bars: 200 nm (A and B) and 100 nm (C_1).

compartment in the vicinity of the assembly sites. Within the viral factories, the two membranes composing the viral envelope would be so closely juxtaposed that they would appear to be a single membrane.

DISCUSSION

Large enveloped DNA viruses like poxviruses and herpesviruses take their membranes by an enwrapping process from cellular cisternae (16, 29, 33, 38, 43). In the present study, we propose that ASFV, another complex DNA virus, uses a similar mechanism to acquire its inner envelope. According to our previous work, the assembly pathway of ASFV is a complex multistep process which is first manifested by the appearence of electron-dense membranous structures within cytoplasmic viral factories. These precursor viral membranes enclose the core material while becoming polyhedral particles by the gradual assembly of the capsid on their convex surfaces (3, 15). As a consequence, the resulting intracellular particles are composed of a core surrounded by two shells, an inner envelope and an outer capsid. The whole process occurs in the cytosol, so that a budding process cannot explain ASFV envelopment. Additionally, this implies that both faces of the viral envelope are exposed to a cytosolic environment. Our model is not, however, topologically consistent with the classical view of the structure of ASFV and of the related iridoviruses, which considers the inner envelope to be a single lipid membrane (7, 10, 20, 41). Cellular membranes are asymmetric structures, with one face exposed to the cytosol and the other exposed to either the luminal or the extracellular space. Assuming that viral membranes are derived from the host cell and respect its topology (19, 26, 40), we first asked whether ASFV is wrapped by a cellular cisterna instead of a single membrane.

The results of the present work, based on both ultrastructural and immunocytochemical EM approaches, support the conclusion that the inner viral envelope is derived from a collapsed two-membraned ER cisterna. Two distinct membranes could be discerned within all intracellular viral forms, from the precursor membrane-like structures onward. However, they appeared so tightly bound that they usually seemed to be a single lipid bilayer. Importantly, the two membranes appeared to be frequently interconnected by loop-like structures at the ends of the precursor viral membranes as well as in open

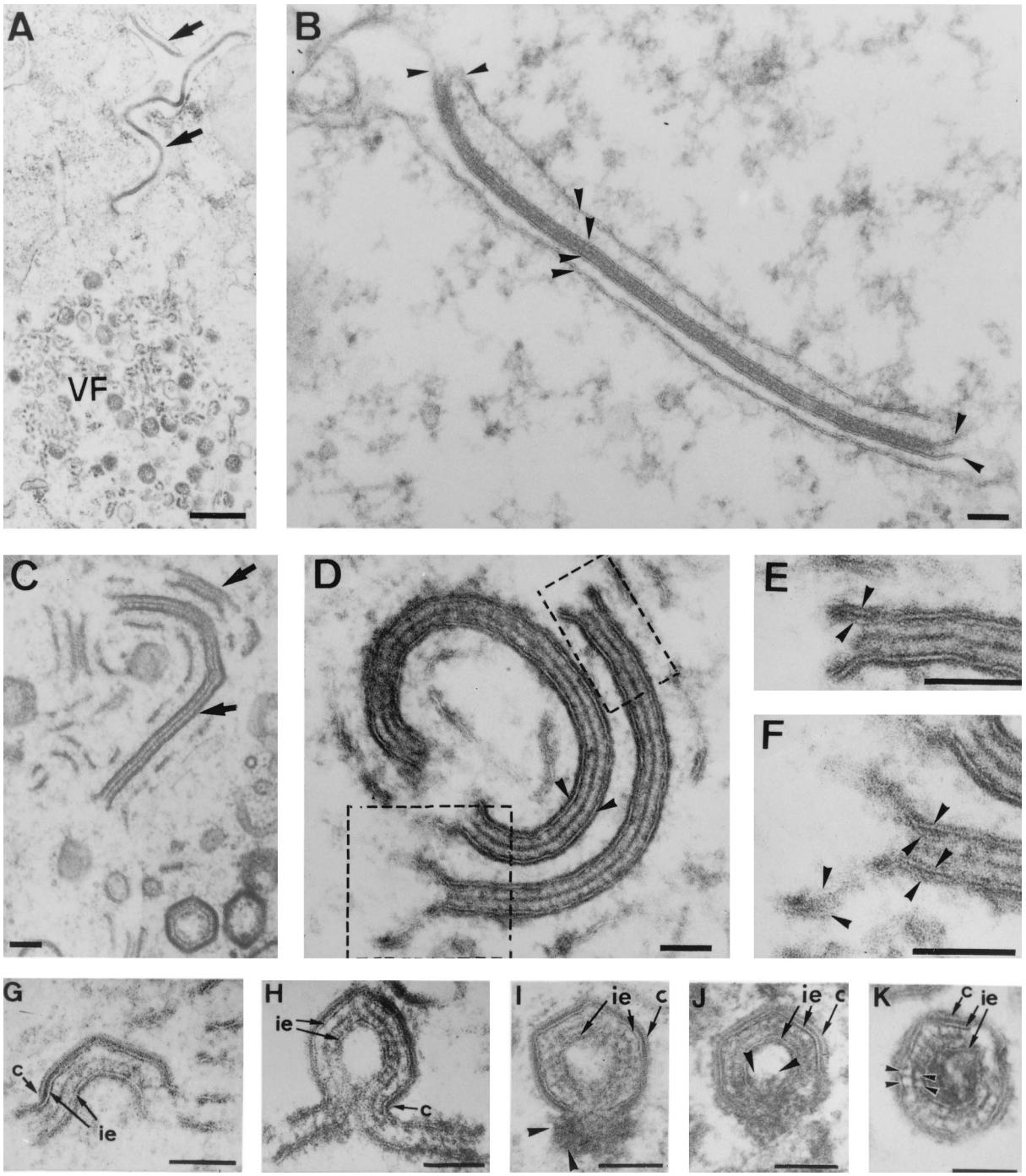

FIG. 6. Assembly of zipper-like structures. Epon sections of viral zipper-like structures present in the bordering areas of the assembly sites (A and B) or within them (C to I). (A and B) Outside the viral factories (VF), these atypical viral intermediates (arrows in panel A) consist of an extended core shell limited by two membrane cisternae (arrowheads in panel B). (C to E) Within the viral factories, closely related zipper-like structures are also found (arrows in panel C). These intermediates are composed by an extended core shell limited by two typical membrane-like structures (arrowheads in panel D). When examined in detail (panels E and F are higher magnifications of the areas delimited in panel D), two apposed lipid membranes (arrowheads) can be discerned within each limiting viral envelope. (G to K) Eventually, the zipper-like structures become polyhedral particles by the progressive formation of a capsid layer (c) on one of the two limiting envelopes (ie). Concomitantly, a nucleoprotein-like material appears to be encapsidated within some double-enveloped particles (arrowheads in panels I and J). Finally, after membrane fusion events, the resulting closed particles contain two inner envelopes encompassing the core shell (K). Note that the core shell is formed by two regular arrays of protein subunits (arrowheads in panel K) separated by a thin electron-dense protein layer. Bars: 500 nm (A) and 100 nm (B to K).

polyhedral assembling virions. Together, these data argue for the cisternal nature of the inner envelope.

Additional support for this model was obtained from experiments involving selective disruption of virus particles. This approach revealed that the outer capsid was resistant to treatments with nonionic detergents but digested with proteinase K. The resulting particles retained the icosahedral symmetry in the first case but not in the second. These results are in agree-

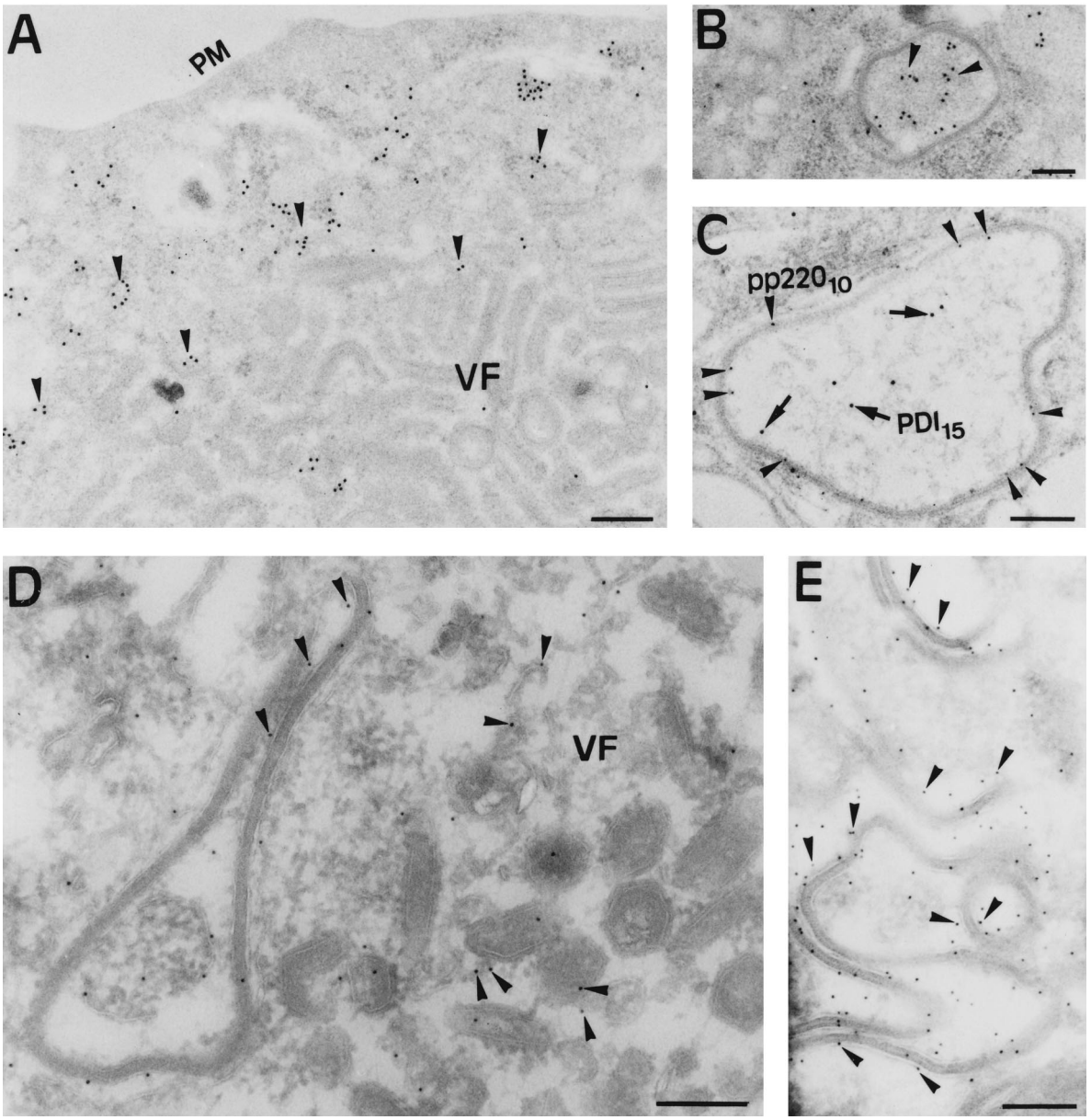

FIG. 7. Immunogold labeling of ER marker proteins in ASFV-infected cells. Vero cells infected with ASFV for 18 h p.i. were processed by freeze-substitution (A to C) or cryosectioning (D and E). (A and B) Ultrathin sections were incubated with a MAb against the luminal ER protein PDI followed by rabbit anti-mouse immunoglobulin G and protein A-gold (diameter, 15 nm). Note that anti-PDI labeling (arrowheads) is essentially excluded from the assembly sites (A) but not from the luminal contents of peripheral zipper-like structures (B). (C) Double labeling of a zipper-like structure with antiserum to polyprotein pp220 followed by protein A-gold (diameter, 10 nm) and with the anti-PDI MAb followed by protein A-gold (diameter, 15 nm). The anti-pp220 labeling (arrowheads) is located within the core shell, while PDI (arrows) is present within the associated cisterna. (D and E) Thawed cryosections were incubated with anti-MERG antiserum followed by protein A-gold (diameter, 10 nm). The labeling is associated with the membranes of marginal zipper-like structures (D and E) and, to a much lesser extent, to viral structures within the viral factories (E). Bars: 500 nm (A) and 200 nm (B to E).

ment with the protein nature of the capsid and confirm its central role in the ASFV morphology (7, 15). By contrast, the inner envelope showed the opposite behavior. It was removed by detergents but not by the proteinase. Importantly, after the proteinase K treatment, two detached membranes became obvious within the inner envelope of highly disrupted particles, which is consistent with the architecture proposed for ASFV.

During the preparation of this communication, a report by Roullier et al. (31) suggested a different structure for the intracellular ASFV particles. On the basis of the electron-lucent appearance alone, these authors interpret the two main shells encompassing the viral core to be lipid membranes. Additionally, in such a model, the capsid is an outermost structure that, surprisingly, is not visible or identified in the reported micrographs. In our opinion, it is well established that the second, outer shell of ASFV and also of the related iridoviruses is an icosahedral capsid made up of protein units, the capsomers, closely packaged in an hexagonal arrangement (Fig. 1C) (2, 7, 10, 20, 41). We have recently shown that this layer is progressively assembled on preexisting membrane-like structures, which concomitantly become polyhedral particles (Fig. 1E and 6G and H) (3). Moreover, its formation can be reversibly inhibited

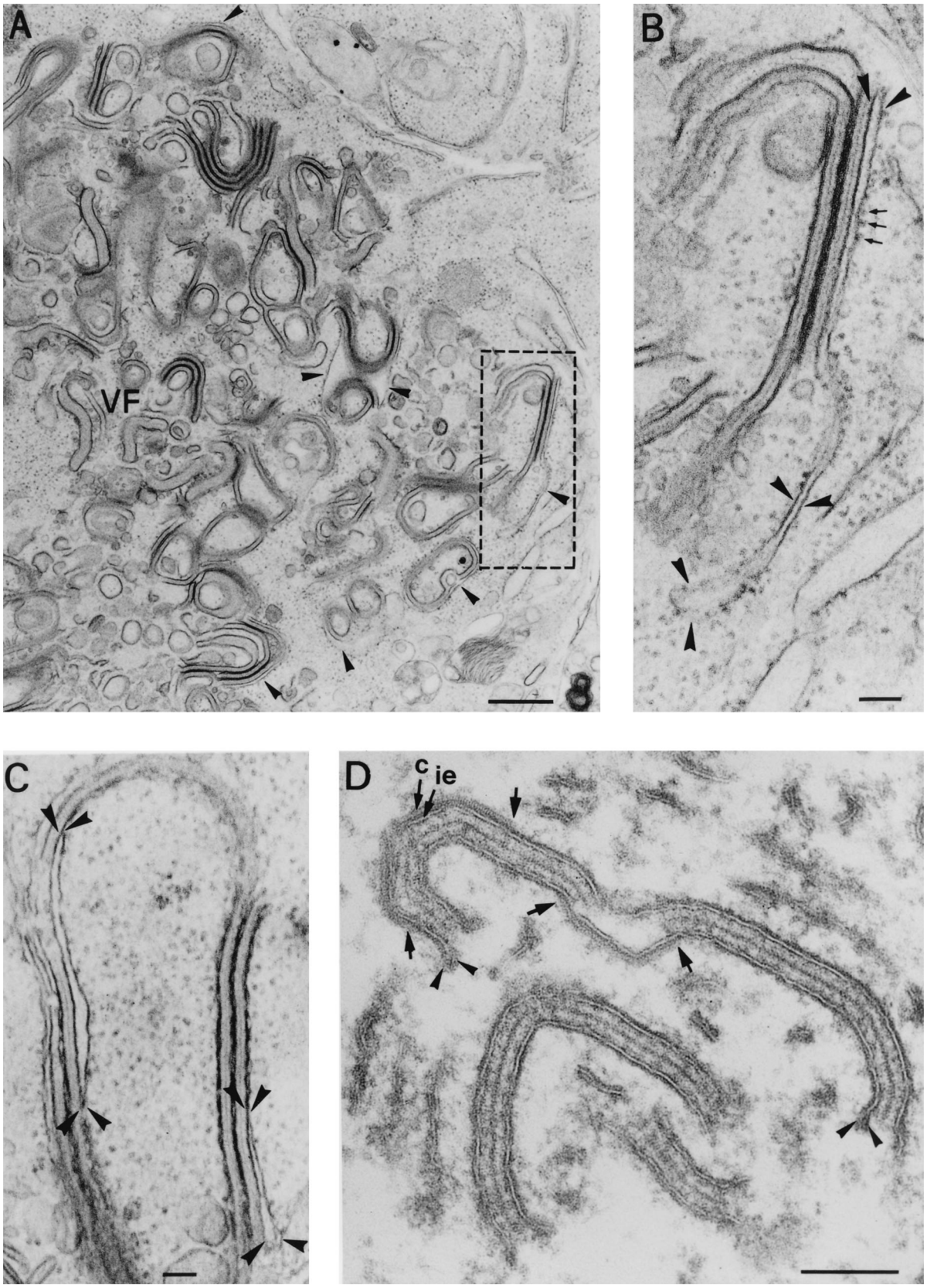

FIG. 8. Origin of the inner envelope of ASFV recombinant vA72. Epon sections of Vero cells infected with recombinant virus vA72 for 18 h in the absence of IPTG (A to C), or treated with the inducer at 18 h p.i. for an 8-h period (D) are shown. (A) Under nonpermissive conditions, the viral factories (VF) show a great accumulation of zipper-like structures and a virtual absence of polyhedral viral structures, as a consequence of the inhibition of capsid formation. In the peripheral areas of the assembly sites, the zipper-like structures appear clearly associated with ER cisternae (arrowheads). (B) Higher magnification of the region delimited in panel

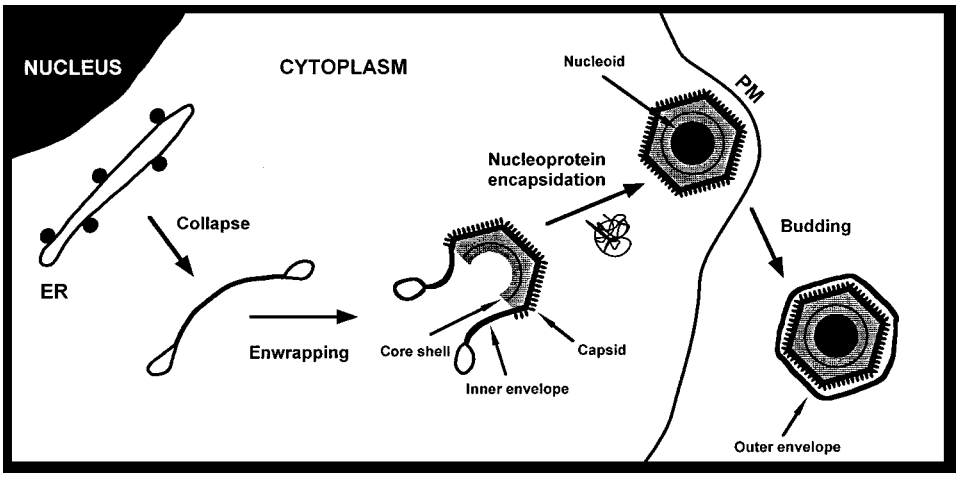

FIG. 9. Model for ASFV assembly. Intracellular ASFV particles acquire their inner envelopes from the ER. The envelopment probably begins by the insertion of viral proteins into the ER membranes and, concomitantly, the exclusion of the host membrane proteins. During this process, the cell compartment would be collapsed to give rise to precursor viral structures formed by two tightly apposed membranes. Subsequently, the capsid would be gradually assembled on one side of the inner envelope whereas the core shell would form beneath the opposite face. At the time the particle is closing, the nucleoprotein material of the nucleoid would become engulfed. Finally, the intracellular particles would release from the cell by budding at the plasma membrane (PM). According to this model, the resulting extracellular ASFV particles would contain three lipid membranes.

with a recombinant virus, vA72, that inducibly expresses the major capsid protein p72 (Fig. 8A to C) (15). In other words, this shell does not exist when p72 expression is inhibited but it can be assembled de novo on the inner envelope after IPTG induction (Fig. 8D). Finally, the present work shows that this layer is resistant to detergent treatments whereas it is digested by proteinase K (Fig. 2). We therefore believe that the outer shell described by Roullier et al. as a lipid membrane is in fact the viral capsid.

An alternative possibility based on both models, i.e., that the capsid is a virus-modified membrane, does not seem probable. On the one hand, the above considerations do not support the presence of a lipid membrane within the capsid layer. On the other hand, such a hypothesis would imply that the capsomers are inserted into a lipid bilayer. However, the major capsid protein p72 lacks transmembrane domains (22) and has been recently characterized by Cobbold et al. as a peripheral membrane protein (8). Such evidence is consistent with our present model.

The second important question analyzed in the present study is the origin of the inner viral envelope. Double-immunofluorescence experiments showed a strong presence of ER and Golgi markers at the limits of the assembly sites but a drastic exclusion of these proteins from the internal areas. At the EM level, morphological and immunocytochemical approaches revealed a close association and even direct continuities between ER membranes and viral intermediates at the periphery of the assembly sites. Collectively, these results indicate that the viral envelopes are derived from ER cisternae and that their transformation into viral intermediates is probably confined to the peripheral areas of the viral factories. This would explain the virtual absence of cell organelles within the assembly sites and the difficulty in detecting direct continuities between cellular and viral membranes (3, 23; see above). In this respect, the immunolabeling data are in agreement with the extended view that the enveloped viruses effectively exclude and replace the host membrane proteins by virus-encoded proteins (26, 40). A study by Brookes et al. (5) showed that during ASFV infection, the viral factory increases in size considerably, conquering new cytoplasmic areas. According to our observations, this fact could be the result of the continued demand for ER membranes during ASFV assembly.

The analysis of the viral zipper-like structures provided a useful approach to understanding the process of envelopment of ASFV. These viral intermediates, which are frequently observed although in small amounts, consist of two adjacent membrane cisternae bound by an extended viral domain structurally similar to the viral core shell (3). In relation to the limiting membrane cisternae, two extreme situations were observed. In the peripheral areas of the viral factories, they appeared as typical ER cisternae with ribosome-attached membranes containing both luminal and membrane ER host proteins. By contrast, within the viral factories, the zipper-like structures appeared limited by typical viral envelopes made up of two closely apposed membranes. This finding suggests, together with the observation of zipper-like structures with partially collapsed ER cisternae during the assembly of recombinant vA72, that the collapse of ER cisternae leads to the formation of the inner viral envelope.

An interesting aspect of the zipper-like structures is the unusual topology of the core shell. Whereas the core shell of normal particles is located between the inner envelope and the nucleoid, in the zipper-like intermediates it is encompassed by lipid membranes. Interestingly, in both cases, this viral domain appears to be composed of two regular arrays of globular subunits separated by a thin electron-dense layer (3) (Fig. 6K).

A. Note how a rough ER cisterna (arrowheads) appears directly bound to an extended viral core shell. The small arrows indicate ribosomes. (C) Partially collapsed ER cisternae associated with zipper-like structures. The arrowheads delimit local extensions where the cisternal structure is still evident. In our interpretation, the collapse would lead to formation of the viral envelopes by the tight apposition of the two limiting lipid bilayers. (D) Detail of a viral factory after an 8-h period of IPTG induction. Under these conditions, the zipper-like structures become polyhedral intermediates by the de novo and gradual assembly of the capsid layer (c) on the inner envelope (ie). The arrows indicate the ends of two capsids assembling on opposite faces of the same zipper-like structure. Note also the presence of membrane loops (arrowheads) at the ends of the viral envelopes. Bars: 500 nm (A) and 100 nm (B to D).

Such a configuration is consistent with the symmetrical features of the zipper-like intermediates but does not explain the polarization of the core shell in normal particles. This difference might reflect the eventual absence of a key viral component(s) during the assembly of the zipper-like structures. In this sense, the finding that these viral forms accumulate when the expression of the capsid protein p72 is inhibited (15) implies that this protein and the process of capsid formation play a role in the polarization of the virus intermediates.

Collectively, the results of this work suggest a model for the assembly of ASFV as presented in Fig. 9. The process probably begins with the insertion of key viral proteins into the ER membranes and the concomitant exclusion of the host cell proteins. Intraluminal interactions between viral membrane proteins would lead to the collapse of the ER cisternae, giving rise to the precursor viral membranous structures. Subsequently, peripheral membrane proteins like p72 (8) would bind to the viral envelope to form the capsid layer on one face, while other membrane-associated proteins such as polyprotein pp220 (3) would form the core shell on the opposite side. Such a model implies a polarization of the collapsed cisternae that needs to be elucidated. One possibility is that distinct viral membrane integral proteins are differently sorted into the outer and inner membranes of the viral envelope. Another possible explanation is that the viral envelope becomes polarized by cooperative interactions between peripheral membrane proteins on local extensions of the collapsed cisterna. In this sense, the progressive assembly of the capsid components and the subsequent bending of the envelope could represent a key event in the generation of asymmetrical viral envelopes. During the late stages of ASFV morphogenesis, the nucleoprotein material of the nucleoid is probably assembled within the particle at the time when it is closing (3). Finally, the intracellular particles would be released to the extracellular space by a budding process at the plasma membrane (4). As a consequence, the resulting ASFV particles would contain three lipid membranes, with the two innermost ones being derived from a collapsed cisterna. Although this model is strongly supported by morphological and immunocytochemical evidence, further efforts will be required to understand the molecular mechanisms involved in crucial events such as the collapse and polarization of the cisternal viral envelope or the encapsidation of the viral genome.

Despite the obvious morphological differences between ASFV and the poxviruses, this assembly model is analogous in some aspects to that described for the intracellular mature form of vaccinia virus (IMV). According to Roos et al. (29), the lipid envelope of IMV consists of two juxtaposed lipid membranes covered by a brush-like array of protein spicules on its convex surface. This envelope is derived from cisternal elements of the intermediate compartment, a specialized region of the ER contiguous with the Gogi complex (38). Importantly, the two apposed membranes of IMV are usually indiscernible but become obvious after protease treatments (38). ASFV and the poxviruses share striking features such as the genome organization (44) or the transcriptional control of gene expression (28). In this context, our present work establishes a new similarity between the two families of complex deoxyviruses. On the other hand, considering the closely related morphology of the iridoviruses and ASFV (7, 41), which was formerly considered to be one of them, it could be predicted that a similar mechanism would also explain their assembly pathway.

ACKNOWLEDGMENTS

We thank M. L. Salas and J. Salas for critical reading of the manuscript. We are very grateful to E. Berger, J. G. Castaño, H.-P. Hauri, D. I. Meyer, J. Rohrer, I. Sandoval, and A. Schweizer for their generous gifts of antibodies. We also thank C. San-Martin and M. Rejas for technical assistance and J. A. Pérez Gracia for skillful help with the photography work.

This study was supported by grants from the Dirección General de Investigación Científica y Técnica (PB96-0902-C02-01), the European community (FAIR-CT97-3441), and Fundación Ramón Areces. Germán Andrés was supported by fellowships from Fundación Rich and Comunidad Autónoma de Madrid, and Ramón García-Escudero was supported by a fellowship from the Comunidad Autónoma de Madrid.

REFERENCES

1. **Alcalde, J., G. Egea, and I. V. Sandoval.** 1994. gp74, a membrane glycoprotein of a cis-Golgi network that cycles through the endoplasmic reticulum and intermediate compartment. J. Cell Biol. **124:**649–665.
2. **Almeida, J. D., A. P. Waterson, and W. Plowright.** 1967. The morphological characteristics of African swine fever virus and its resemblance to Tipula iridescent virus. Arch. Gesamte Virusforsch. **20:**392–396.
3. **Andrés, G., C. Simón-Mateo, and E. Viñuela.** 1997. Assembly of African swine fever virus: role of polyprotein pp220. J. Virol. **71:**2331–2341.
4. **Breese, S. S., Jr., and C. J. DeBoer.** 1966. Electron microscope observation of African swine fever virus in tissue culture cells. Virology **28:**420–428.
5. **Brookes, S. M., L. K. Dixon, and R. M. E. Parkhouse.** 1996. Assembly of African swine fever virus: quantitative ultrastructural analysis *in vitro* and *in vivo*. Virology **224:**84–92.
6. **Carrascosa, A. L., M. del Val, J. F. Santarén, and E. Viñuela.** 1985. Purification and properties of African swine fever virus. J. Virol. **54:**337–344.
7. **Carrascosa, J. L., J. M. Carazo, A. L. Carrascosa, N. García, A. Santisteban, and E. Viñuela.** 1984. General morphology and capsid fine structure of African swine fever virus particles. Virology **132:**160–172.
8. **Cobbold C., J. T. Whittle, and T. Wileman.** 1996. Involvement of the endoplasmic reticulum in the assembly and envelopment of African swine fever virus. J. Virol. **70:**8382–8390.
9. **Costa, J. V.** 1990. African swine fever virus, p. 247–270. *In* G. Darai (ed.), Molecular biology of iridoviruses. Kluwer Academic Publishers, Boston, Mass.
10. **Darcy-Tripier, F., M. V. Nermut, J. Braunwald, and L. D. Williams.** 1984. The organization of frog virus 3 as revealed by freeze-etching. Virology **138:** 287–299.
11. **Del Val, M., J. L. Carrascosa, and E. Viñuela.** 1986. Glycosylated components of African swine fever virus. Virology **152:**39–49.
12. **Dixon, L. K., D. Rock, and E. Viñuela.** 1995. African swine fever-like particles. Virus taxonomy: classification and nomenclature of viruses. Arch. Virol. **10**(Suppl.)**:**92–94.
13. **Enjuanes, L., A. L. Carrascosa, M. A. Moreno, and E. Viñuela.** 1976. Titration of African swine fever (ASF) virus. J. Gen. Virol. **32:**471–477.
14. **García-Beato, R., M. L. Salas, E. Viñuela, and J. Salas.** 1992. Role of the host cell nucleus in the replication of African swine fever virus DNA. Virology **188:**637–649.
15. **García-Escudero, R., G. Andrés, F. Almazán, and E. Viñuela.** 1998. Inducible gene expression from African swine fever virus recombinants: analysis of the major capsid protein p72. J. Virol. **72:**3185–3195.
16. **Gershon, A. A., D. L. Sherman, Z. L. Zhu, C. A. Gabel, R. T. Ambron, and M. D. Gershon.** 1994. Intracellular transport of newly synthesized varicella-zoster virus: final envelopment in the *trans*-Golgi network. J. Virol. **68:**6372–6390.
17. **González, A., A. Talavera, J. M. Almendral, and E. Viñuela.** 1986. Hairpin loop structure of African swine fever virus DNA. Nucleic Acids Res. **14:** 6835–6844.
18. **Griffiths, G.** 1993. Fine structure immunocytochemistry. Springer-Verlag KG, Heidelberg, Germany.
19. **Griffiths, G., and P. Rottier.** 1992. Cell biology of viruses that assemble along the biosynthetic pathway. Semin. Cell Biol. **3:**367–381.
20. **Heppell, J., and L. Berthiaume.** 1992. Ultrastructure of lymphocystis disease virus (LCDV) as compared to frog virus 3 (FV_3) and chilo iridescent virus (CIV): effects of enzymatic digestions and detergent degradations. Arch. Virol. **125:**215–226.
21. **Liou, W., H. J. Geuze, and J. W. Slot.** 1996. Improving structural integrity of cryosections for immunogold labeling. Histochem. Cell. Biol. **106:**41–58.
22. **López-Otín, C., J. M. P. Freije, F. Parra, E. Méndez, and E. Viñuela.** 1990. Mapping and sequence of the gene coding for protein p72, the major capsid protein of African swine fever virus. Virology **175:**477–484.
23. **Moura Nunes, J. F., J. D. Vigario, and A. M. Terrinha.** 1975. Ultraestructural study of African swine fever virus replication in cultures of swine bone marrow cells. Arch. Virol. **49:**59–66.
24. **Nieto, A., E. Mira, and J. G. Castaño.** 1990. Transcriptional regulation of rat liver protein disulphide-isomerase gene by insulin and in diabetes. Biochem. J. **267:**317–323.
25. **Pagano, R. E., M. A. Sepanski, and O. C. Martin.** 1989. Molecular trapping of a fluorescent ceramide analogue at the Golgi apparatus of fixed cells: interaction with endogenous lipids provideds a trans-Gogi marker for both

light and electron microscopy. J. Cell Biol. **109:**2067–2079.
26. **Pettersson, R. F.** 1991. Protein localization and virus assembly at intracellular membranes. Curr. Top. Microbiol. Immunol. **170:**67–106.
27. **Plutner, H., A. D. Cox, S. Pind, R. Khosravi-Far, J. R. Bourne, R. Schwaninger, C. J. Der, and W. E. Balch.** 1991. Rab1b regulates vesicular transport between the endoplasmic reticulum and successive Golgi compartments. J. Cell Biol. **115:**31–43.
28. **Rodriguez, J. M., M. L. Salas, and E. Viñuela.** 1996. Intermediate class of mRNAs in African swine fever virus. J. Virol. **70:**8584–8589.
29. **Roos, N., M. Cyrklaf, S. Cudmore, R. Blasco, J. Krinjse-Locker, and G. Griffiths.** 1996. A novel immunogold cryoelectron microscopic approach to investigate the structure of the intracellular and extracellular forms of vaccinia virus. EMBO J. **15:**2343–2355.
30. **Roth, J., and E. C. Berger.** 1982. Immunocytochemical localization of galactosyltransferase in Hela cells: codistribution with thiamine pyrophosphatase in trans-Golgi cisternae. J. Cell Biol. **92:**223–229.
31. **Roullier, I., S. M. Brookes, A. D. Hyatt, M. Windsor, and T. Wileman.** 1998. African swine fever virus is wrapped by the endoplasmic reticulum. J. Virol. **72:**2373–2387.
32. **Sanz, A., B. García-Barreno, M. L. Nogal, E. Viñuela, and L. Enjuanes.** 1985. Monoclonal antibodies specific for African swine fever virus proteins. J. Virol. **54:**199–206.
33. **Schmelz, M., B. Sodeik, M. Ericson, E. J. Wolffe, H. Shida, G. Hiller, and G. Griffiths.** 1994. Assembly of vaccinia virus: the second wrapping cisterna is derived from the *trans*-Golgi network. J. Virol. **68:**130–147.
34. **Schweizer, A., J. A. M. Fransen, T. Bächi, L. Ginsel, and H. P. Hauri.** 1988. Identification, by a monoclonal antibody, of a 53 kDa protein associated with a tubulo-vesicular compartment at the *cis*-side of the Golgi apparatus. J. Cell Biol. **107:**1643–1653.
35. **Schweizer, A., J. Rohrer, J. W. Slot, H. J. Geuze, and S. Kornfeld.** 1995. Reassessment of the subcellular localization of p63. J. Cell Sci. **108:**2477–2485.
36. **Simón-Mateo, C., G. Andrés, and E. Viñuela.** 1993. Polyprotein prcessing in African swine fever virus: a novel gene expression strategy for a DNA virus. EMBO J. **12:**2977–2987.
37. **Simón-Mateo, C., G. Andrés, F. Almazán, and E. Viñuela.** 1997. Proteolytic processing in African swine fever virus: evidence for a new structural polyprotein, pp62. J. Virol. **71:**5799–5804.
38. **Sodeik, B., R. W. Doms, M. Ericsson, G. Hiller, C. E. Machamer, W. van't Hof, G. van Meer, B. Moss, and G. Griffiths.** 1993. Assembly of Vaccinia virus: role of the intermediate compartment between the endoplasmic reticulum and the Golgi stacks. J. Cell Biol. **121:**521–541.
39. **Sogo, J. M., J. M. Almendral, A. Talavera, and E. Viñuela.** 1984. Terminal and internal inverted repetitions in African swine fever virus DNA. Virology **133:**271–275.
40. **Stephens, E. B., and R. W. Compans.** 1988. Assembly of animal viruses at cellular membranes. Annu. Rev. Microbiol. **42:**489–516.
41. **Stolz, D.** 1973. The structure of icosahedral cytoplasmic deoxyriboviruses. II. An alternative model. J. Ultrastruct. Res. **43:**58–74.
42. **Tooze, J., H. F. Kern, S. D. Fuller, and K. E. Howell.** 1989. Condensation-sorting events in the rough endoplasmic reticulum of exocrine pancreatic cells. J. Cell Biol. **109:**35–50.
43. **Tooze, J., M. Hollinshead, B. Reis, K. Radsak, and H. Kern.** 1991. Progeny vaccinia and cytomegalovirus particles utilize early endosomal cisternae for their envelopes. Eur. J. Cell Biol. **60:**163–178.
44. **Viñuela, E.** 1987. Molecular biology of African swine fever virus, p. 31–49. *In* Y. Becker (ed.), African swine fever. Nijhoff, Boston, Mass.
45. **Yáñez, R. J., J. M. Rodríguez, M. L. Nogal, L. Yuste, C. Enriquez, J. F. Rodríguez, and E. Viñuela.** 1995. Analysis of the complete nucleotide sequence of African swine fever virus. Virology **208:**249–278.
46. **Yuan, L., J. G. Barriocanal, J. S. Bonifacino, and I. V. Sandoval.** 1987. Two integral membrane proteins located in the cis-midle and transport of the Golgi system acquire sialyted N-linked carbohydrates and display different turnovers and sensitivity of cAMP-dependent phosphorylation. J. Cell Biol. **105:**215–227.